

$\phi \rightarrow \pi^0 \eta \gamma$ and $\phi \rightarrow \pi^0 \pi^0 \gamma$ decays and Mixing Between Low and High Mass Scalar Mesons

T. Teshima,* I. Kitamura, and N. Morisita
*Department of Natural Sciences,
Chubu University, Kasugai 487-8501, Japan*

Radiative decays $\phi \rightarrow \eta \pi^0 \gamma$ and $\phi \rightarrow \pi^0 \pi^0 \gamma$ are studied assuming that these decays are caused through the intermediate $a_0(980)\gamma$ and $f_0(980)\gamma$ states, respectively. Fitting the experimental data of the $\eta \pi^0$ and $\pi^0 \pi^0$ invariant mass spectrum in the decays $\phi \rightarrow \eta \pi^0 \gamma$ and $\phi \rightarrow \pi^0 \pi^0 \gamma$, it is shown that the processes $\phi \rightarrow a_0 \gamma$ and $\phi \rightarrow f_0 \gamma$ are dominated by the $K^+ K^-$ loop interaction rather than the contact $\phi a_0(f_0) \gamma$ one both for the non-derivative and derivative SPP coupling. The experimental data of $\Gamma[\phi \rightarrow f_0 \gamma]/\Gamma[\phi \rightarrow a_0 \gamma]$ predicts that $g_{f_0 K \bar{K}}/g_{a_0 K \bar{K}} \sim 2$. Considering the effects of the mixing between low mass scalar $q\bar{q}q\bar{q}$ states and high mass scalar $q\bar{q}$ states to these coupling constants $g_{f_0 K \bar{K}}$ and $g_{a_0 K \bar{K}}$, one suggests that the mixing is rather large.

PACS numbers: 12.39.Mk, 12.40.Yx, 13.66.Jn

I. INTRODUCTION

For a long time, the radiative decays of the ϕ to $\pi^0 \eta \gamma$ and $\pi^0 \pi^0 \gamma$ have been analyzed, assuming that the decays $\phi \rightarrow \pi^0 \eta(\pi^0) \gamma$ proceed through the $\phi \rightarrow a_0(f_0) \gamma$ decays, to reveal the structure of the light scalar mesons $a_0(980)$ and $f_0(980)$ [1, 2, 3]. These analyses are performed assuming the charged $K^+ K^-$ loop diagram in the coupling $\phi a_0(f_0) \gamma$ and the contact (vector dominance) $\phi a_0(f_0) \gamma$ interaction. In this work, we analyze the data for the $\pi^0 \eta$ and $\pi^0 \pi^0$ invariant mass spectrum in $\phi \rightarrow \pi^0 \eta \gamma$ and $\phi \rightarrow \pi^0 \pi^0 \gamma$ decays given in recent precise experiment [4], assuming charged $K^+ K^-$ loop diagram and contact $\phi f_0(a_0) \gamma$ interaction. For the S (scalar meson)- P (pseudo-scalar meson)- P (pseudo-scalar meson) interactions appeared in these decaying processes, we consider the cases non-derivative interaction and derivative one, latter of which is adopted in the literature [3]. The result obtained in our present analysis shows that these processes are caused through the $K^+ K^-$ loop diagram dominantly.

When the $K^+ K^-$ loop diagram is dominant in the decays $\phi \rightarrow f_0 \gamma \rightarrow \pi^0 \pi^0 \gamma$ and $\phi \rightarrow a_0 \gamma \rightarrow \pi^0 \eta \gamma$, the value of the ratio $g_{f_0 K \bar{K}}/g_{a_0 K \bar{K}}$ is obtained from the experimental ratio $\Gamma(\phi \rightarrow a_0 \gamma)/\Gamma(\phi \rightarrow f_0 \gamma)$, that is the rather large value $g_{f_0 K \bar{K}}/g_{a_0 K \bar{K}} \sim 2$. These coupling constant strengths depend on the structure of the scalar mesons, that is, these scalar mesons are constituted of $q\bar{q}$ or $q\bar{q}q\bar{q}$, or are mixing states of $q\bar{q}$ and $q\bar{q}q\bar{q}$. Authors in Ref. [1] argue that the data of $\phi \rightarrow a_0(f_0) \gamma \rightarrow \pi^0 \eta(\pi^0) \gamma$ decays gives evidence in favor of the $q\bar{q}q\bar{q}$ nature for the scalar $a_0(980)$ and $f_0(980)$ mesons, and authors in Ref. [2] argue the matter of mixing between $q\bar{q}$ and $q\bar{q}q\bar{q}$ states.

Recent many literature (refer to the "Note on scalar mesons" in [5]) suggest that the low mass scalar nonet ($f_0(600)$, $K_0^*(800)$, $a_0(980)$, $f_0(980)$) are $q\bar{q}q\bar{q}$ state and the high mass scalar mesons ($a_0(1450)$, $K_0^*(1430)$, $f_0(1370)$, $f_0(1500)$, $f_0(1710)$) are conventional $L = 1$ $q\bar{q}$ nonet plus one glueball. We assume a strong mixing between low mass and high mass scalar mesons to explain the fact that the high $L = 1$ $q\bar{q}$ scalar nonet are so high compared to other $L = 1$ $q\bar{q}$ 1^{++} and 2^{++} mesons [6, 7]. Assuming that the coupling strengths causing the mixing between $I = 1$ $a_0(980)$ and $a_0(1450)$, $I = 1/2$ $K_0^*(800)$ and $K_0^*(1430)$ and $I = 0$ ($f_0(600)$, $f_0(980)$) and ($f_0(1370)$, $f_0(1500)$, $f_0(1710)$) are same, we analyzed the $S \rightarrow PP$ decays using derivative SPP couplings [8]. Fitting the various experimental SPP decay widths, we obtained the mixing angle between $a_0(980)$ and $a_0(1450)$ as $\sim 9^\circ$. In our previous work [9], we analyzed the $\Gamma(\phi \rightarrow f_0 \gamma)$ and $\Gamma(\phi \rightarrow a_0 \gamma)$ assuming the contact (vector dominance) coupling for the $a_0 \phi \gamma$ and $f_0 \phi \gamma$ interaction and using the mixing strength obtained in previous work [8], and then suggested the importance of the

*Electronic address: teshima@isc.chubu.ac.jp

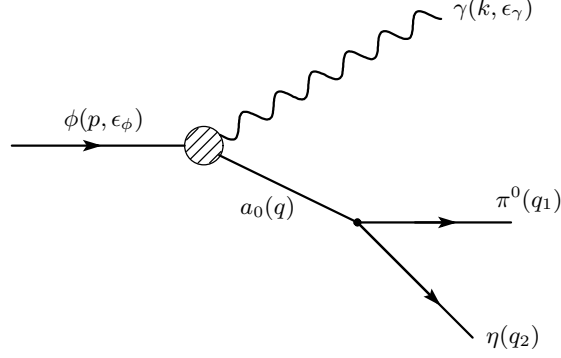


FIG. 1: Diagram for the decay $\phi \rightarrow a_0(980)\gamma \rightarrow \pi^0\eta\gamma$

mixing effect for the explanation of the rather large ratio $\Gamma(\phi \rightarrow f_0\gamma)/\Gamma(\phi \rightarrow a_0\gamma)$.

In section 2, we analyze the data for $\pi^0\eta$ and $\pi^0\pi^0$ invariant mass spectrum of the $dBR(\phi \rightarrow \pi^0\pi^0\gamma)/dq$ and $dBR(\phi \rightarrow \pi^0\eta\gamma)/dq$ assuming the intermediate scalar states $f_0(980)$ and $a_0(980)$. In this analyses, we consider the contact and K^+K^- loop interaction for $\phi f_0(a_0)\gamma$ coupling, in cases of derivative and non-derivative SPP coupling. In section 3, we reanalyze our mass formula for low mass nonet scalar and high mass nonet scalar + glueball adopting the new mass data of $K_0^*(800)$ [5]. In section 4, we express the SPP coupling constants $g_{a_0\pi\pi}$, $g_{f_0\pi\pi}$ etc. using the mixing parameters between low and high mass scalar mesons. We pursue the best fit analyses for the $S \rightarrow PP$ decay data using the mixing parameters obtained in section 3 for both non-derivative and derivative SPP interactions, and then obtain the best fit $g_{f_0K\bar{K}}$ etc. Comparing the best fit $g_{f_0K\bar{K}}$ etc. with the values obtained from the $\phi \rightarrow f_0(a_0)\gamma$ decays, we suggest that the non-derivative coupling is reasonable than the derivative one and the mixing between $q\bar{q}$ and $q\bar{q}\bar{q}$ is rather large.

II. ANALYSIS OF THE $\phi \rightarrow \pi^0\eta\gamma$ AND $\phi \rightarrow \pi^0\pi^0\gamma$ DECAYS

A. $\phi \rightarrow \pi^0\eta\gamma$ decay

Firstly, we consider the decay $\phi \rightarrow a_0(980)\gamma \rightarrow \pi^0\eta\gamma$ shown in Fig. 1. The invariant mass distribution of the branching ratio $dBR(\phi \rightarrow a_0(980)\gamma \rightarrow \pi^0\eta\gamma)/dm$ is expressed as (refer to first paper in Ref. [1])

$$\frac{dBR(\phi \rightarrow a_0\gamma \rightarrow \pi^0\eta\gamma)}{dm} = \frac{2m^2}{\pi} \frac{1}{\Gamma_\phi} \frac{\Gamma(\phi \rightarrow a_0\gamma : m)\Gamma(a_0 \rightarrow \pi^0\eta : m)}{|D_{a_0}(m^2)|^2}, \quad (1)$$

where Γ_ϕ is a decay width of ϕ and $1/D_{a_0}(m^2)$ represents the propagator of the intermediate state a_0 ,

$$D_{a_0}(m^2) = m^2 - m_{a_0}^2 - im_{a_0}\Gamma_{a_0}. \quad (2)$$

$\Gamma(a_0 \rightarrow \pi^0\eta : m)$ is the decay width on the virtual mass m of intermediate a_0 defined as $m = \sqrt{q_0^2 - \mathbf{q}^2}$,

$$\begin{aligned} \Gamma(a_0 \rightarrow \pi^0\eta : m) &= \frac{g_{a_0\pi\eta}^2}{8\pi m^2} \frac{\sqrt{(m^2 - (m_\pi + m_\eta)^2)(m^2 - (m_\pi - m_\eta)^2)}}{2m} \\ &\times \begin{cases} 1 & \text{for non-derivative coupling,} \\ \left(\frac{m^2 - m_\pi^2 - m_\eta^2}{2} \right)^2 & \text{for derivative coupling,} \end{cases} \end{aligned} \quad (3)$$

where coupling constant $g_{a_0\pi\eta}$ is defined as

$$M(a_0(q) \rightarrow \pi^0(q_1) + \eta(q_2)) = g_{a_0\pi\eta} \times \begin{cases} 1 & \text{for non-derivative coupling,} \\ q_1 \cdot q_2 & \text{for derivative coupling.} \end{cases} \quad (4)$$

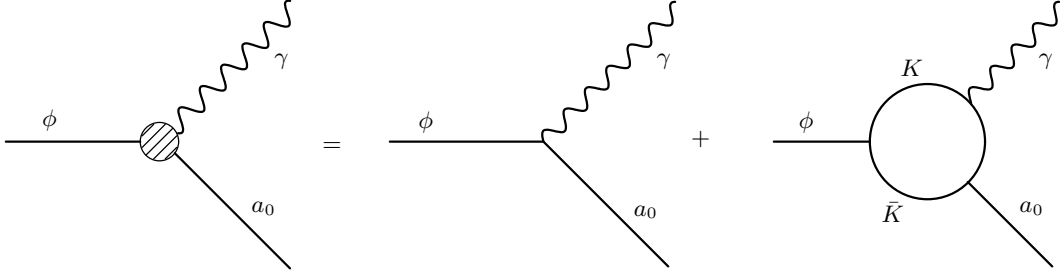


FIG. 2: Diagrams for the contact and K^+K^- loop coupling contributing to $g_{\phi a_0 \gamma}(m)$

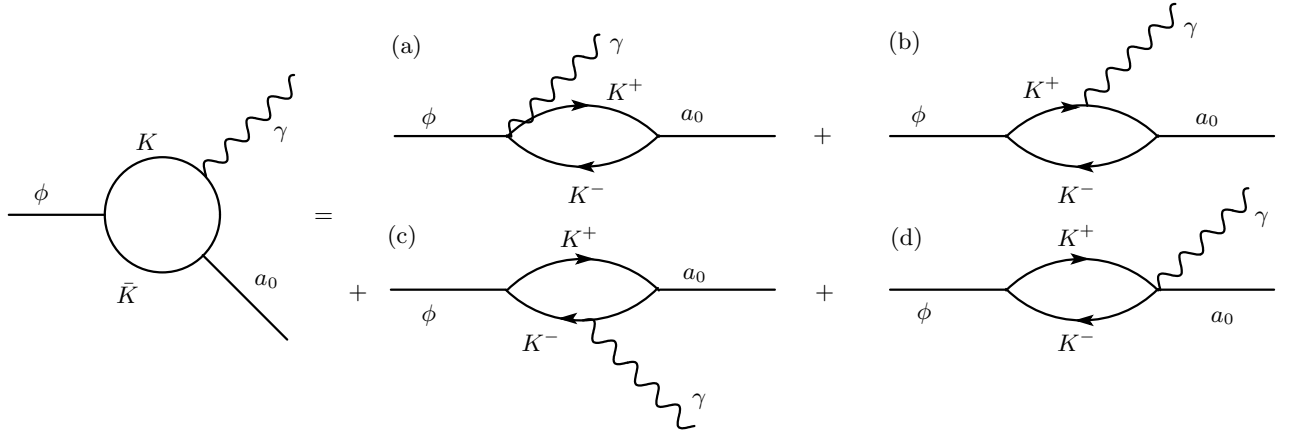


FIG. 3: Diagrams for the K^+K^- loop coupling contributing to $g_{\phi a_0 \gamma}(m)$

$\Gamma(\phi \rightarrow a_0 \gamma : m)$ is the decay width on the virtual mass $m = \sqrt{q_0^2 - \mathbf{q}^2}$ of intermediate state a_0 ,

$$\Gamma(\phi \rightarrow a_0 \gamma : m) = \frac{\alpha}{3} g_{\phi a_0 \gamma}^2(m) \left(\frac{m_\phi^2 - m^2}{2m_\phi} \right)^3, \quad (5)$$

where coupling constant $g_{\phi a_0 \gamma}(m)$ is defined as

$$M(\phi(p, \epsilon_\phi) \rightarrow a_0(q) + \gamma(k, \epsilon_\gamma)) = e g_{\phi a_0 \gamma}(m) (p \cdot k \epsilon_\phi \cdot \epsilon_\gamma - p \cdot \epsilon_\gamma k \cdot \epsilon_\phi). \quad (6)$$

For the coupling $g_{\phi a_0 \gamma}(m)$, contact interaction and K^+K^- loop interaction contribute as shown in Fig. 2, and then $g_{\phi a_0 \gamma}(m)$ is expressed as

$$g_{\phi a_0 \gamma}(m) = g_{\phi a_0 \gamma}^{\text{contact}} + g_{\phi a_0 \gamma}^{K\bar{K}\text{loop}}(m). \quad (7)$$

$g_{\phi a_0 \gamma}^{K\bar{K}\text{loop}}(m)$ is calculated for non-derivative $a_0 K^+ K^-$ coupling by many authors (N. N. Achasov *et al.* and F. E. Close *et al.* in [1]) considering three diagrams (a), (b) and (c) shown in Fig. 3, as

$$g_{\phi a_0 \gamma}^{K\bar{K}\text{loop}}(m) = \frac{g_{\phi K \bar{K}} g_{a_0 K \bar{K}}}{2\pi^2 i m_K^2} I(a, b). \quad \text{for non-derivative coupling} \quad (8)$$

The quantities a, b are defined as $a = m_\phi^2/m_K^2$, $b = m^2/m_K^2$ and $I(a, b)$ arisen from the loop integral is

$$I(a, b) = \frac{1}{2(a-b)} - \frac{2}{(a-b)^2} \left\{ f\left(\frac{1}{b}\right) - f\left(\frac{1}{a}\right) \right\} + \frac{a}{(a-b)^2} \left\{ g\left(\frac{1}{b}\right) - g\left(\frac{1}{a}\right) \right\}, \quad (9)$$

where

$$\begin{aligned} f(x) &= \begin{cases} -\left(\sin^{-1}\left(\frac{1}{2\sqrt{x}}\right)\right)^2, & x > \frac{1}{4} \\ \frac{1}{4} \left[\log \frac{\eta_+}{\eta_-} - i\pi\right]^2, & x < \frac{1}{4} \end{cases} \\ g(x) &= \begin{cases} \sqrt{4x-1} \sin^{-1}\left(\frac{1}{2\sqrt{x}}\right), & x > \frac{1}{4} \\ \frac{1}{2} \sqrt{1-4x} \left[\log \frac{\eta_+}{\eta_-} - i\pi\right], & x < \frac{1}{4} \end{cases} \\ \eta_\pm &= \frac{1}{2x} (1 \pm \sqrt{1-4x}). \end{aligned} \quad (10)$$

The coupling constant $g_{\phi K \bar{K}}$ is defined as

$$M(\phi(p, \epsilon^\phi) \rightarrow K^+(q_1) + K^-(q_2)) = g_{\phi K \bar{K}} \epsilon_\mu^\phi (q_1^\mu - q_2^\mu), \quad (11)$$

and decay width is expressed as

$$\Gamma(\phi \rightarrow K^+ + K^-) = \frac{g_{\phi K \bar{K}}^2}{4\pi} \frac{2}{3m_\phi^2} \left(\frac{m_\phi^2}{4} - m_K^2 \right)^{3/2}. \quad (12)$$

The coupling constant $g_{\phi K \bar{K}}$ is estimated using the experimental data $\Gamma(\phi \rightarrow K^+ + K^-) = 2.10 \pm 0.05 \text{ MeV}$ [5] as

$$g_{\phi K \bar{K}} = 4.55 \pm 0.06. \quad (13)$$

For the $a_0 K^+ K^-$ coupling, $g_{a_0 K \bar{K}}$ is defined by the similar expression as Eq. (4)

$$M(a_0(q) \rightarrow K^+(q_1) + K^-(q_2)) = g_{a_0 K \bar{K}} \times \begin{cases} 1 & \text{for non-derivative coupling,} \\ q_1 \cdot q_2 & \text{for derivative coupling.} \end{cases} \quad (4')$$

For derivative coupling of $a_0 K^+ K^-$, $K^+ K^-$ loop diagram contribution $g_{\phi a_0 \gamma}^{K \bar{K} \text{ loop}}(m)$ is calculated by D. Black *et al.* [2] considering four diagrams (a), (b), (c) and (d) shown in Fig. 3, as

$$g_{\phi a_0 \gamma}^{K \bar{K} \text{ loop}}(m) = \frac{g_{\phi K \bar{K}} g_{a_0 K \bar{K}}}{2\pi^2 i m_K^2} \frac{2m_K^2 - m^2}{2} I(a, b) \quad \text{for derivative coupling.} \quad (8')$$

Using Eqs. (2), (3), (5), (7), (8), (8'), we parameterize Eq. (1) as

$$\begin{aligned} \frac{dBR(\phi \rightarrow a_0 \gamma \rightarrow \pi^0 \eta \gamma)}{dm} &= G_1 \frac{|G_2 + \frac{1}{i} \left[\frac{2m_K^2 - m^2}{2} \right] I(a, b)|^2}{|G_2 + \frac{1}{i} \left[\frac{2m_K^2 - m_a^2}{2} \right] I(a, b_0)|^2} \left(\frac{m_\phi^2 - m^2}{m_\phi^2 - m_a^2} \right)^3 \frac{m_a}{m} \\ &\times \frac{m_a^2 \Gamma_a^2}{(m^2 - m_a^2)^2 + m_a^2 \Gamma_a^2} \sqrt{\frac{(m^2 - (m_\eta + m_\pi)^2)(m^2 - (m_\eta - m_\pi)^2)}{(m_a^2 - (m_\eta + m_\pi)^2)(m_a^2 - (m_\eta - m_\pi)^2)}}, \end{aligned} \quad (14)$$

where G_1, G_2, b_0 are defined as

$$\begin{aligned} G_1 &= \frac{2}{\pi \Gamma_\phi \Gamma_a^2} \Gamma(\phi \rightarrow a_0 \gamma : m_a) \Gamma(a_0 \rightarrow \eta \pi^0 : m_a), \\ G_2 &= g_{\phi \gamma a}^{\text{contact}} / \left(\frac{g_{\phi K \bar{K}} g_{a_0 K \bar{K}}}{2\pi^2 m_K^2} \right), \\ b_0 &= \frac{m_a^2}{m_K^2}, \end{aligned} \quad (15)$$

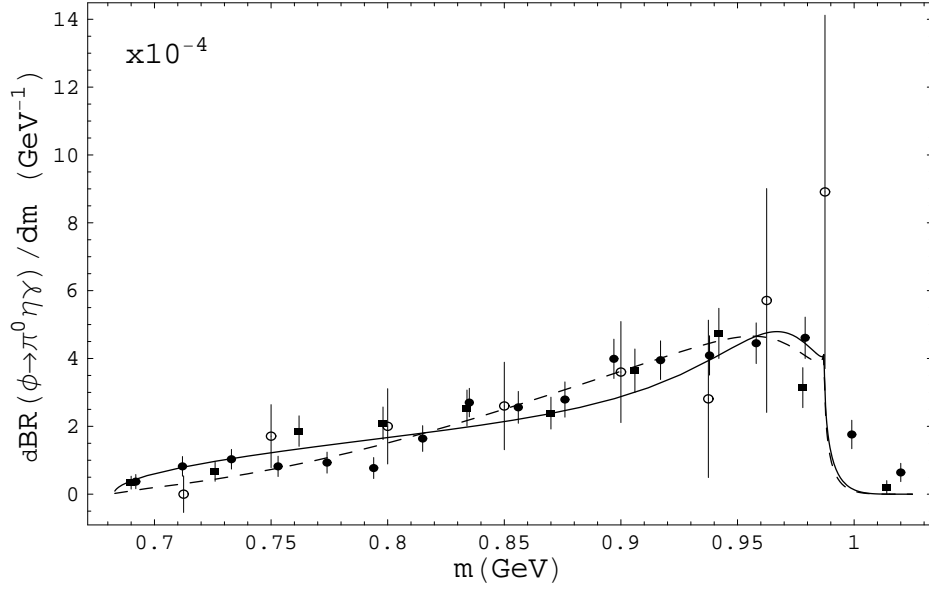


FIG. 4: $dBR(\phi \rightarrow \pi^0\eta\gamma)/dm$ (in unit of GeV^{-1}) as a function of the π^0 - η invariant mass m (in GeV^{-1}). Solid line shows the best fitted curve for the non-derivative SPP coupling interaction and the dashed line shows the best fitted curve for the derivative one. Experimental data indicated by circles are from the SND collaboration in Ref. [4], and those by filled circles and filled squares are from KLEO collaboration in Ref. [4].

and factors $\left[\frac{2m_K^2 - m_a^2}{2}\right]$ and $\left[\frac{2m_K^2 - m_a^2}{2}\right]$ are replaced to 1 for non-derivative SPP coupling. $\Gamma(a_0 \rightarrow \eta\pi^0, m_a)$ and $\Gamma(\phi \rightarrow a_0\gamma, m_a)$ are defined in Eq. (3) and (5) settling $m \rightarrow m_a$. We fit the Eq. (14) varying the parameters G_1 and G_2 using the experimental data from the SND collaboration and KLEO collaboration in Ref. [4]. Best-fitted curves are shown in Fig. 4; solid line for non-derivative SPP coupling and dashed line for derivative SPP coupling are obtained for the choice of the parameters G_1 and G_2 as $G_1 = 4.1 \times 10^{-4}\text{GeV}^{-1}$, $G_2 = -0.16$ for non-derivative coupling and $G_1 = 3.9 \times 10^{-4}\text{GeV}^{-1}$, $G_2 = 0.08$ for derivative coupling. For these choices, the estimated $BR(\phi \rightarrow \pi^0\eta\gamma)$ are estimated as

$$G_1 = 4.1 \times 10^{-4}\text{GeV}^{-1}, G_2 = -0.16, BR(\phi \rightarrow \pi^0\eta\gamma) = 7.03 \times 10^{-5} \quad \text{for non-derivative coupling,} \quad (16)$$

$$G_1 = 3.9 \times 10^{-4}\text{GeV}^{-1}, G_2 = 0.08, BR(\phi \rightarrow \pi^0\eta\gamma) = 7.12 \times 10^{-5} \quad \text{for derivative coupling.} \quad (16')$$

Estimated value for $BR(\phi \rightarrow \pi^0\eta\gamma)$ is consistent with the experimental data $BR^{\text{exp}}(\phi \rightarrow \pi^0\eta\gamma) = (8.3 \pm 0.5) \times 10^{-5}$ [4, 5]. Also, estimated value of G_1 is consistent with the value evaluated from the experimental data (Ref. [5]) using the relation Eq. (15),

$$G_1^{\text{exp}} = \frac{2}{\pi\Gamma_a} BR^{\text{exp}}(\phi \rightarrow a_0\gamma : m_a) BR^{\text{exp}}(a_0 \rightarrow \eta\pi^0 : m_a) = (5.96 \pm 2.47) \times 10^{-4}\text{GeV}^{-1}.$$

Furthermore G_2 is very small compared to $|I(a, b_0)| = 0.902$ for $m_a = 0.985$ GeV, then we can suppose that the K^+K^- loop contribution is dominant in the $\phi \rightarrow \pi^0\eta\gamma$ decay. Supposing that the decay $\phi \rightarrow a_0\gamma$ is caused through only the K^+K^- loop interaction, we obtain the result,

$$\Gamma(\phi \rightarrow a_0\gamma) = \frac{\alpha}{3} \left| \frac{g_{\phi K\bar{K}} g_{a_0 K\bar{K}}}{2\pi^2 m_K^2} \left[\frac{2m_K^2 - m_a^2}{2} \right] I(a, b_0) \right|^2 \left(\frac{m_\phi^2 - m_a^2}{2m_\phi} \right)^3, \quad (17)$$

where the factor $\left[\frac{2m_K^2 - m_a^2}{2}\right]$ is replaced to 1 for the non-derivative coupling. Using the value Eq. (13) of $g_{\phi K\bar{K}}$

and the experimental value $\Gamma(\phi \rightarrow a_0\gamma) = (0.323 \pm 0.029) \times 10^{-3} \text{MeV}$ in Ref.[5], we obtain the result

$$g_{a_0 K \bar{K}} = \begin{cases} 2.18 \pm 0.12 \text{ GeV}, & \text{for non-derivative coupling} \\ 9.04 \pm 0.50 \text{ GeV}^{-1}. & \text{for derivative coupling} \end{cases} \quad (18)$$

Using relations Eqs. (15), (3), (17) and estimated results Eq. (16), (16'), (18), we obtained the values for $g_{a_0\pi\eta}$,

$$g_{a_0\pi\eta} = \begin{cases} 1.89 \pm 0.75 \text{ GeV}, & \text{for non-derivative coupling} \\ 5.79 \pm 2.32 \text{ GeV}^{-1}. & \text{for derivative coupling} \end{cases} \quad (18')$$

B. $\phi \rightarrow \pi^0\pi^0\gamma$ decay

For the decay $\phi \rightarrow f_0\gamma \rightarrow \pi^0\pi^0\gamma$, the invariant mass distribution of the branching ratio $dBR(\phi \rightarrow f_0\gamma \rightarrow \pi^0\pi^0\gamma)/dm$ is expressed similar to Eq. (14) for the case $\phi \rightarrow a_0\gamma \rightarrow \pi^0\eta\gamma$ as

$$\begin{aligned} \frac{dBR(\phi \rightarrow f_0\gamma \rightarrow \pi^0\pi^0\gamma)}{dm} &= G_1 \frac{|G_2 + \frac{1}{i} \left[\frac{2m_K^2 - m^2}{2} \right] I(a, b)|^2}{|G_2 + \frac{1}{i} \left[\frac{2m_K^2 - m_f^2}{2} \right] I(a, b_0)|^2} \left(\frac{m_\phi^2 - m^2}{m_\phi^2 - m_f^2} \right)^3 \frac{m_f}{m} \\ &\times \frac{m_f^2 \Gamma_f^2}{(m^2 - m_f^2)^2 + m_f^2 \Gamma_f^2} \sqrt{\frac{m^2 - 4m_\pi^2}{m_f^2 - 4m_\pi^2}}, \end{aligned} \quad (19)$$

where G_1, G_2, b_0 are defined as

$$\begin{aligned} G_1 &= \frac{2}{\pi \Gamma_\phi \Gamma_f^2} \Gamma(\phi \rightarrow f_0\gamma : m_f) \Gamma(f_0 \rightarrow \pi^0\pi^0 : m_f), \\ G_2 &= g_{\phi\gamma f}^{\text{contact}} / \left(\frac{g_{\phi K \bar{K}} g_{f_0 K \bar{K}}}{2\pi^2 m_K^2} \right), \\ b_0 &= \frac{m_f^2}{m_K^2}. \end{aligned} \quad (20)$$

Here, $\Gamma(f_0 \rightarrow \pi^0\pi^0 : m_f)$ and $\Gamma(\phi \rightarrow f_0\gamma : m_f)$ are expressed as

$$\begin{aligned} \Gamma(f_0 \rightarrow \pi^0\pi^0 : m_f) &= \frac{g_{f_0\pi\pi}^2}{16\pi m_f^2} \frac{\sqrt{m_f^2 - 4m_\pi^2}}{2} \\ &\times \begin{cases} 1 & \text{for non-derivative coupling,} \\ \left(\frac{m_f^2 - 2m_\pi^2}{2} \right)^2 & \text{for derivative coupling,} \end{cases} \end{aligned} \quad (21)$$

where coupling constant $g_{f_0\pi\pi}$ is defined as

$$M(f_0(q) \rightarrow \pi^0(q_1) + \pi^0(q_2)) = \frac{1}{2} g_{f_0\pi\pi} \times \begin{cases} 1 & \text{for non-derivative coupling,} \\ q_1 \cdot q_2 & \text{for derivative coupling,} \end{cases} \quad (22)$$

and

$$\Gamma(\phi \rightarrow f_0\gamma : m_f) = \frac{\alpha}{3} g_{\phi f_0\gamma}^2(m_f) \left(\frac{m_\phi^2 - m_f^2}{2m_\phi} \right)^3, \quad (23)$$

$$g_{\phi f_0\gamma}(m_f) = g_{\phi f_0\gamma}^{\text{contact}} + \frac{g_{\phi K \bar{K}} g_{f_0 K \bar{K}}}{2\pi^2 i m_K^2} \left[\frac{2m_K^2 - m_f^2}{2} \right] I(a, b_0). \quad (24)$$

In Eq. (24), factor $\left[\frac{2m_K^2 - m_f^2}{2} \right]$ is replaced to 1 for non-derivative coupling. $g_{f_0 K \bar{K}}$ is defined in the similar equation as Eq. (22),

$$M(f_0(q) \rightarrow K^+(q_1) + K^-(q_2)) = g_{f_0 K \bar{K}} \times \begin{cases} 1 & \text{for non-derivative coupling,} \\ q_1 \cdot q_2 & \text{for derivative coupling,} \end{cases} \quad (22')$$

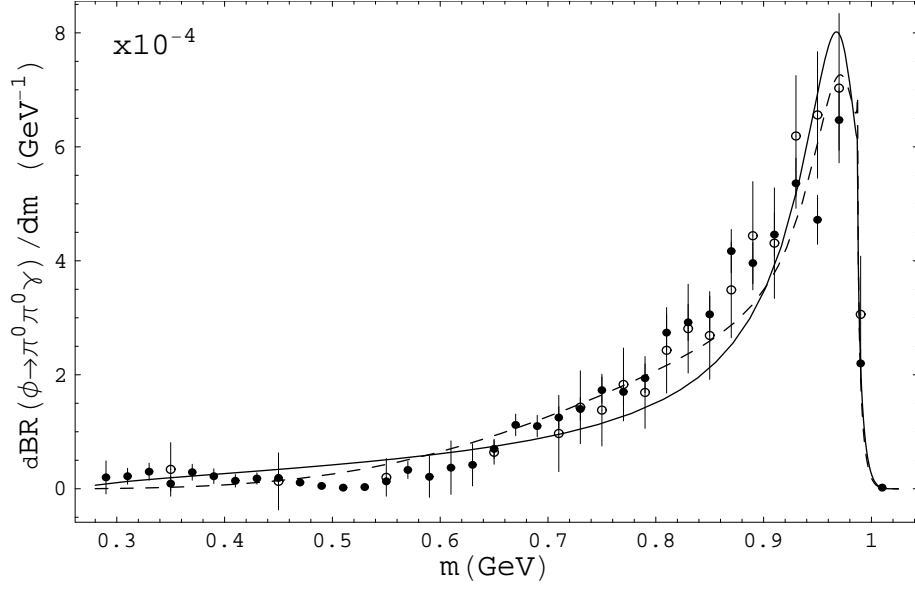


FIG. 5: $dBR(\phi \rightarrow \pi^0\pi^0\gamma)/dm$ (in unit of GeV^{-1}) as a function of the π^0 - π^0 invariant mass m (in GeV^{-1}). Solid line shows the best fitted curve for the non-derivative coupling and the dashed line shows the best fitted curve for the derivative one. Experimental data indicated by circles are from the SND collaboration in Ref. [4], and those by filled circles are from KLEO collaboration in Ref. [4].

We fit the Eq. (19) using the experimental data from the SND and KLEO collaboration in Ref. [4], and obtain the best-fitted curves shown in Fig. 5; solid line for non-derivative coupling and dashed line for derivative one. The choice of the parameters G_1 and G_2 for these best fit and estimated value for $BR(\phi \rightarrow \pi^0\pi^0\gamma)$ are obtained as

$$G_1 = 7.1 \times 10^{-4} \text{GeV}^{-1}, \quad G_2 = 0.001, \quad BR(\phi \rightarrow \pi^0\pi^0\gamma) = 1.06 \times 10^{-4} \quad \text{for non-derivative coupling,} \quad (25)$$

$$G_1 = 6.9 \times 10^{-4} \text{GeV}^{-1}, \quad G_2 = 0.055, \quad BR(\phi \rightarrow \pi^0\pi^0\gamma) = 1.08 \times 10^{-4} \quad \text{for derivative coupling.} \quad (25')$$

Estimated value for $BR(\phi \rightarrow \pi^0\pi^0\gamma)$ is consistent with the experimental data $BR^{\text{exp}}(\phi \rightarrow \pi^0\pi^0\gamma) = (1.09 \pm 0.06) \times 10^{-4}$ [4, 5], and estimated value of G_1 is consistent with the value evaluated from the experimental data (Ref. [5]),

$$G_1^{\text{exp}} = \frac{2}{\pi\Gamma_f} BR^{\text{exp}}(\phi \rightarrow f_0\gamma : m_f) BR^{\text{exp}}(f_0 \rightarrow \pi^0\pi^0 : m_f) = (10.0 \pm 4.8) \times 10^{-4} \text{GeV}^{-1}.$$

As the case for the decay $\phi \rightarrow \pi^0\eta\gamma$, contact $g_{\phi f_0\gamma}$ interaction (G_2) is very small compared to $|I(a, b_0)| = 0.783$ for $m_f = 0.980$ GeV, then one can suppose that the K^+K^- loop contribution is dominant in the $\phi \rightarrow \pi^0\pi^0\gamma$ decay. We suppose the $\phi \rightarrow f_0\gamma$ decay is caused from the K^+K^- loop interaction, then can estimate the coupling constant $g_{a_0 K \bar{K}}$ from the relation

$$\Gamma(\phi \rightarrow f_0\gamma) = \frac{\alpha}{3} \left| \frac{g_{\phi K \bar{K}} g_{f_0 K \bar{K}}}{2\pi^2 m_K^2} \left[\frac{2m_K^2 - m_f^2}{2} \right] I(a, b_0) \right|^2 \left(\frac{m_\phi^2 - m_f^2}{2m_\phi} \right)^3, \quad (26)$$

where the factor $\left[\frac{2m_K^2 - m_f^2}{2} \right]$ is replaced to 1 for the non-derivative coupling. Using the value Eq. (13) of $g_{\phi K \bar{K}}$ and the experimental value $\Gamma(\phi \rightarrow f_0\gamma) = (0.323 \pm 0.029) \times 10^{-3} \text{MeV}$ in Ref.[5], we obtain the result

$$g_{f_0 K \bar{K}} = \begin{cases} 4.72 \pm 0.82 \text{ GeV}, & \text{for non-derivative coupling} \\ 20.0 \pm 0.50 \text{ GeV}^{-1}. & \text{for derivative coupling} \end{cases} \quad (27)$$

Using relations Eqs. (20), (21), (26) and estimated results (25), (25'), (27), we obtained the values for $g_{f_0\pi\pi}$,

$$g_{f_0\pi\pi} = \begin{cases} 1.12 \pm 0.69 \text{ GeV}, & \text{for non-derivative coupling} \\ 2.43 \pm 1.50 \text{ GeV}^{-1}. & \text{for derivative coupling} \end{cases} \quad (27')$$

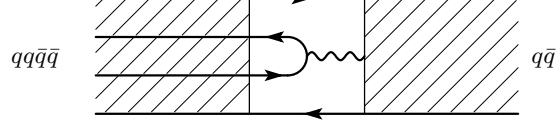


Fig. 6 OZI rule allowed graph for $qq\bar{q}\bar{q}$ and $q\bar{q}$ states transition

The rather large value of the ratio $g_{f_0 K \bar{K}}/g_{a_0 K \bar{K}} \sim 2$ suggests that the a_0 and f_0 scalar mesons are not the pure $qq\bar{q}\bar{q}$ states but there exist the mixing (inter-mixing) between $qq\bar{q}\bar{q}$ and $q\bar{q}$ scalar mesons. Furthermore, the existence of the coupling $g_{f_0 \pi \pi}$ suggest the intra mixing between $qq\bar{q}\bar{q}$ $f_0(600)$ and $f_0(980)$ scalar mesons.

III. MIXING BETWEEN LOW AND HIGH MASS SCALAR MESONS

In this section, we review the mixing among the low mass scalar, high mass scalar and glueball discussed in our previous work [7, 8]. The $qq\bar{q}\bar{q}$ scalar $SU(3)$ nonet S_a^b are represented by the quark triplet q_a and anti-quark triplet \bar{q}^a as

$$S_b^a \sim \epsilon^{acd} q_c q_d \epsilon_{bef} \bar{q}^e \bar{q}^f \quad (28)$$

and have the following flavor configuration [10], [6]:

$$\begin{aligned} \bar{d}\bar{s}s u, \frac{1}{\sqrt{2}}(\bar{d}\bar{s}ds - \bar{s}\bar{u}su), \bar{s}\bar{u}ds &\Longleftrightarrow a_0^+, a_0^0, a_0^- \\ \bar{d}\bar{s}ud, \bar{s}\bar{u}ud, \bar{u}\bar{d}s u, \bar{u}\bar{d}ds &\Longleftrightarrow \kappa^+, \kappa^0, \bar{\kappa}^0, \kappa^- \\ \frac{1}{\sqrt{2}}(\bar{d}\bar{s}ds + \bar{s}\bar{u}su) &\Longleftrightarrow f_{NS} \sim f_0(980) \\ \bar{u}\bar{d}ud &\Longleftrightarrow f_{NN} \sim f_0(600) \end{aligned}$$

The high mass scalar mesons $S_b'^a$ are the ordinary $SU(3)$ nonet

$$S_b'^a \sim \bar{q}^a q_b.$$

The inter-mixing between $qq\bar{q}\bar{q}$ and $q\bar{q}$ states may be large, because the transition between $qq\bar{q}\bar{q}$ and $q\bar{q}$ states is caused by the OZI rule allowed diagram shown in fig. 6. Considering the above flavor configuration for $qq\bar{q}\bar{q}$ states, the expression for this transition is suggested as

$$\begin{aligned} L_{\text{int}} = & \lambda_{01} [a_0^+ a_0'^- + a_0^- a_0'^+ + a_0^0 a_0'^0 + K_0^{*+} K_0'^{-*} + K_0^{*-} K_0'^{*-} + K_0^{*0} K_0'^{*0} + \bar{K}_0^{*0} \bar{K}_0'^{*0} \\ & + \sqrt{2} f_{NN} f_N' + f_{NS} f_N' + \sqrt{2} f_{NS} f_S']. \end{aligned} \quad (29)$$

The parameter λ_{01} represents the strength of the inter-mixing and can be considered as rather large. When we represent the $I = 1$ pure $qq\bar{q}\bar{q}$ and $q\bar{q}$ states by $a_0(980)$ and $a_0(1450)$, and masses for these states by $m_{a_0(980)}^2$ and $m_{a_0(1450)}^2$, the mass matrix is represented as

$$\begin{pmatrix} m_{a_0(980)}^2 & \lambda_{01} \\ \lambda_{01} & m_{a_0(1450)}^2 \end{pmatrix}. \quad (30)$$

Diagonalising this mass matrix, we can get the masses for the physical states $a_0(980)$ and $a_0(1450)$ represented as mixing states of $a_0(980)$ and $a_0(1450)$;

$$\begin{aligned} a_0(980) &= \cos \theta_a \overline{a_0(980)} - \sin \theta_a \overline{a_0(1450)}, \\ a_0(1450) &= \sin \theta_a \overline{a_0(980)} + \cos \theta_a \overline{a_0(1450)}. \end{aligned} \quad (31)$$

Mixing angle θ_a and before mixing state masses $m_{a_0(980)}^2$ and $m_{a_0(1450)}^2$ are represented by the inter-mixing parameter λ_{01} as

$$\begin{aligned} \epsilon_a &= \frac{m_{a_0(1450)}^2 - m_{a_0(980)}^2}{2} - \sqrt{\left(\frac{m_{a_0(1450)}^2 - m_{a_0(980)}^2}{2}\right)^2 - \lambda_{01}^2}, \\ \theta_a &= \tan^{-1} \frac{\epsilon_a}{\lambda_{01}} \\ m_{a_0(1450)}^2 &= \sqrt{m_{a_0(1450)}^2 + \epsilon_a}, \quad m_{a_0(980)}^2 = \sqrt{m_{a_0(980)}^2 - \epsilon_a}, \end{aligned} \quad (32)$$

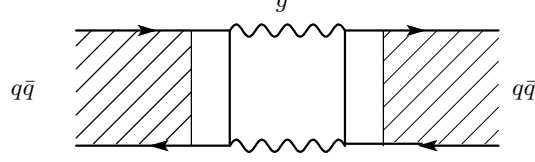


Fig. 7 OZI rule suppression graph for $q\bar{q} - q\bar{q}$ transition.

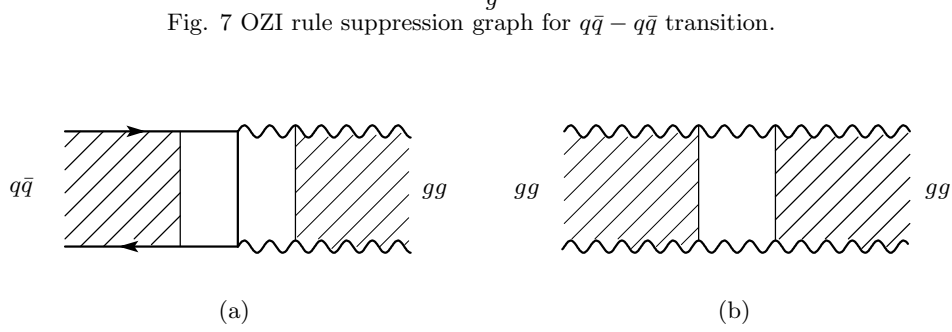


Fig. 8 Transition graph between (a) $q\bar{q}$ and gg , and (b) gg and gg .

where $m_{a_0(980)}$ and $m_{a_0(1450)}$ are the masses of the states $a_0(980)$ and $a_0(1450)$.

Similarly, for the $I = 1/2$ $K_0^*(800)$ and $K_0^*(1430)$ mesons, the mass matrix is represented as

$$\begin{pmatrix} m_{K_0^*(800)}^2 & \lambda_{01} \\ \lambda_{01} & m_{K_0^*(1430)}^2 \end{pmatrix}, \quad (33)$$

where $m_{K_0^*(800)}$ and $m_{K_0^*(1430)}$ are the masses of pure $q\bar{q}q\bar{q}$ and $q\bar{q}$ states $\overline{K_0^*(800)}$ and $\overline{K_0^*(1430)}$. The physical states $K_0^*(800)$ and $K_0^*(1430)$ are written by the before mixing states $\overline{K_0^*(800)}$ and $\overline{K_0^*(1430)}$ and mixing angle θ_K as

$$\begin{aligned} K_0^*(800) &= \cos \theta_K \overline{K_0^*(800)} - \sin \theta_K \overline{K_0^*(1430)}, \\ K_0^*(1430) &= \sin \theta_K \overline{K_0^*(800)} + \cos \theta_K \overline{K_0^*(1430)}. \end{aligned} \quad (34)$$

Mixing angle θ_K and before mixing state masses $m_{K_0^*(800)}$ and $m_{K_0^*(1430)}$ are represented by the inter-mixing parameter λ_{01} as

$$\begin{aligned} \epsilon_K &= \frac{m_{K_0^*(1430)}^2 - m_{K_0^*(800)}^2}{2} - \sqrt{\left(\frac{m_{K_0^*(1430)}^2 - m_{K_0^*(800)}^2}{2}\right)^2 - \lambda_{01}^2}, \\ \theta_K &= \tan^{-1} \frac{\epsilon_K}{\lambda_{01}} \\ m_{K_0^*(1430)} &= \sqrt{m_{K_0^*(1430)}^2 + \epsilon_K}, \quad m_{K_0^*(800)} = \sqrt{m_{K_0^*(800)}^2 - \epsilon_K}, \end{aligned} \quad (35)$$

where $m_{K_0^*(800)}$ and $m_{K_0^*(1430)}$ are the masses of the physical states $K_0^*(800)$ and $K_0^*(1430)$.

Next, we consider the mixing between $I = 0$ low and high mass scalar mesons. Among the $I = 0, L = 1$ $q\bar{q}$ scalar mesons, there are the intra-mixing weaker than the inter-mixing, caused from the transition between themselves represented by the OZI rule suppression graph shown in Fig. 7, and furthermore the mixing between the $q\bar{q}$ scalar meson and the glueball caused from the transition represented by the graph shown in Fig. 8(a). Thus, the mass matrix for these $I = 0, L = 1$ $q\bar{q}$ scalar mesons and glueball is represented as

$$\begin{pmatrix} m_{N'}^2 + 2\lambda_1 & \sqrt{2}\lambda_1 & \sqrt{2}\lambda_G \\ \sqrt{2}\lambda_1 & m_{S'}^2 + \lambda_1 & \lambda_G \\ \sqrt{2}\lambda_G & \lambda_G & \lambda_{GG} \end{pmatrix}, \quad (36)$$

$$m_{N'}^2 = m_{a_0(1450)}^2, \quad m_{S'}^2 = 2m_{K_0^*(1430)}^2 - m_{a_0(1450)}^2,$$

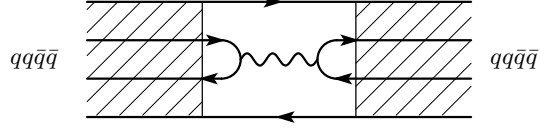


Fig. 9. OZI suppression graph for $qq\bar{q}\bar{q} - qq\bar{q}\bar{q}$ transition.

where λ_1 is the transition strength among the $I = 0$ $q\bar{q}$ mesons, λ_G is the transition strength between $q\bar{q}$ and glueball gg and λ_{GG} is the pure glueball mass square. For the light $I = 0$ $qq\bar{q}\bar{q}$ scalar mesons, there are the intra-mixing caused from the transition between themselves represented by the OZI rule suppression graph shown in Fig. 9, and the mass matrix for these $I = 0$ $qq\bar{q}\bar{q}$ scalar meson is represented as

$$\begin{pmatrix} m_{NN}^2 + \lambda_0 & \sqrt{2}\lambda_0 \\ \sqrt{2}\lambda_0 & m_{NS}^2 + 2\lambda_0 \end{pmatrix}, \quad (37)$$

$$m_{NN}^2 = 2m_{K_0^*(800)}^2 - m_{a_0(980)}^2, \quad m_{NS}^2 = m_{a_0(980)}^2,$$

where λ_0 represents the transition strength between $I = 0$ $qq\bar{q}\bar{q}$ mesons.

The inter- and intra-mixing among $I = 0$ low mass and high mass scalar mesons and glueball is expressed by the overall mixing mass matrix as

$$\begin{pmatrix} m_{NN}^2 + \lambda_0 & \sqrt{2}\lambda_0 & \sqrt{2}\lambda_{01} & 0 & 0 \\ \sqrt{2}\lambda_0 & m_{NS}^2 + 2\lambda_0 & \lambda_{01} & \sqrt{2}\lambda_{01} & 0 \\ \sqrt{2}\lambda_{01} & \lambda_{01} & m_{N'}^2 + 2\lambda_1 & \sqrt{2}\lambda_1 & \sqrt{2}\lambda_G \\ 0 & \sqrt{2}\lambda_{01} & \sqrt{2}\lambda_1 & m_{S'}^2 + \lambda_1 & \lambda_G \\ 0 & 0 & \sqrt{2}\lambda_G & \lambda_G & \lambda_{GG} \end{pmatrix}. \quad (38)$$

Diagonalising this mass matrix, we obtain the eigenvalues of low mass and high mass scalar mesons $I = 0$ states $f_0(600)$, $f_0(980)$, $f_0(1370)$, $f_0(1500)$ and $f_0(1710)$. The eigenstates of these scalar mesons are represented as follows;

$$\begin{pmatrix} f_0(600) \\ f_0(980) \\ f_0(1370) \\ f_0(1500) \\ f_0(1710) \end{pmatrix} = [R_{f_0(M)I}] \begin{pmatrix} f_{NN} \\ f_{NS} \\ f_{N'} \\ f_{S'} \\ f_G \end{pmatrix}, \quad (39)$$

$$[R_{f_0(M)I}] = \begin{pmatrix} R_{f_0(600)NN} & R_{f_0(600)NS} & R_{f_0(600)N'} & R_{f_0(600)S'} & R_{f_0(600)G} \\ R_{f_0(980)NN} & R_{f_0(980)NS} & R_{f_0(980)N'} & R_{f_0(980)S'} & R_{f_0(980)G} \\ R_{f_0(1370)NN} & R_{f_0(1370)NS} & R_{f_0(1370)N'} & R_{f_0(1370)S'} & R_{f_0(1370)G} \\ R_{f_0(1500)NN} & R_{f_0(1500)NS} & R_{f_0(1500)N'} & R_{f_0(1500)S'} & R_{f_0(1500)G} \\ R_{f_0(1710)NN} & R_{f_0(1710)NS} & R_{f_0(1710)N'} & R_{f_0(1710)S'} & R_{f_0(1710)G} \end{pmatrix}.$$

Using the inter-mixing parameter λ_{01} and the mass values, $m_{a_0(980)} = (0.9848 \pm 0.0012)\text{GeV}$, $m_{a_0(1450)} = (1.474 \pm 0.019)\text{GeV}$, $m_{K_0^*(800)} = (0.841 \pm 0.030)\text{GeV}$ and $m_{K_0^*(1430)} = (1.414 \pm 0.006)\text{GeV}$, we obtained the mixing angles θ_a , θ_K and before mixing states masses $m_{\frac{a_0(980)}{a_0(1450)}}$, $m_{\frac{K_0^*(800)}{K_0^*(1430)}}$ from the relations (32) and (35). Using the values of $m_{N'}^2$, $m_{S'}^2$, m_{NN}^2 and m_{NS}^2 obtained from the second equations in Eqs.(36) and (37), and parameters λ_0 , λ_1 , λ_G and λ_{GG} , we diagonalize the mass matrix Eq(38). When we fit the eigenvalues obtained to the following experimental mass values [5],

$$\begin{aligned} m_{f_0(600)} &= 0.80 \pm 0.40\text{GeV}, \quad m_{f_0(980)} = 0.980 \pm 0.010\text{GeV}, \\ m_{f_0(1370)} &= 1.350 \pm 0.150\text{GeV}, \quad m_{f_0(1500)} = 1.507 \pm 0.005\text{GeV}, \\ m_{f_0(1710)} &= 1.718 \pm 0.006\text{GeV}, \end{aligned} \quad (40)$$

we obtain the allowed values for λ_0 , λ_1 , λ_G and λ_{GG} . We tabulated the θ_a , θ_K , λ_0 , λ_1 , λ_G , λ_{GG} , and $R_{f_0(980)NN}$, $R_{f_0(980)NS}$, $R_{f_0(980)N'}$, $R_{f_0(980)S'}$, $R_{f_0(980)G}$ for the various values of λ_{01} in the Table I.

IV. COUPLING CONSTANT g_{SPP} AND MIXING BETWEEN $qq\bar{q}\bar{q}$ AND $q\bar{q}$ SCALAR MESONS

In this section, we first express the g_{SPP} 's by the mixing angle θ_a , θ_K and mixing parameters R_{f_0NS} etc. Next, we obtain the values of the g_{SPP} using the various $S \rightarrow PP$ decay widths and compare these values with the ones

$\lambda_{01}(\text{GeV}^2)$	$\theta_a(^{\circ})$	$\theta_K(^{\circ})$	$\lambda_0(\text{GeV}^2)$	$\lambda_1(\text{GeV}^2)$	$\lambda_G(\text{GeV}^2)$	$\lambda_{GG}(\text{GeV}^2)$
	$R_{f_0(980)NN}$	$R_{f_0(980)NS}$	$R_{f_0(980)N'}$	$R_{f_0(980)S'}$	$R_{f_0(980)G}$	
0.20	9.7 ± 0.5	9.0 ± 0.5	0.018 ± 0.009	0.275 ± 0.007	0.04 ± 0.04	$(1.152 \pm 0.008)^2$
	-0.023 ± 0.014	-0.972 ± 0.002	0.065 ± 0.006	0.226 ± 0.004	-0.010 ± 0.010	
0.25	12.3 ± 0.6	11.4 ± 0.6	0.032 ± 0.010	0.264 ± 0.008	0.05 ± 0.05	$(1.512 \pm 0.007)^2$
	-0.027 ± 0.026	-0.954 ± 0.003	0.086 ± 0.008	0.284 ± 0.005	-0.016 ± 0.016	
0.30	15.0 ± 0.8	13.8 ± 0.8	0.050 ± 0.009	0.252 ± 0.009	0.04 ± 0.04	$(1.512 \pm 0.008)^2$
	-0.046 ± 0.024	-0.932 ± 0.004	0.110 ± 0.009	0.341 ± 0.006	-0.016 ± 0.016	
0.35	17.8 ± 1.0	16.4 ± 1.0	0.072 ± 0.012	0.233 ± 0.008	0.05 ± 0.05	$(1.511 \pm 0.008)^2$
	-0.065 ± 0.025	-0.902 ± 0.007	0.140 ± 0.012	0.401 ± 0.007	-0.024 ± 0.024	
0.40	20.8 ± 1.2	19.1 ± 1.2	0.104 ± 0.012	0.213 ± 0.009	0.05 ± 0.05	$(1.509 \pm 0.006)^2$
	-0.094 ± 0.021	-0.864 ± 0.010	0.178 ± 0.014	0.461 ± 0.007	-0.028 ± 0.028	
0.45	24.2 ± 1.6	22.1 ± 1.5	0.146 ± 0.014	0.178 ± 0.007	0.04 ± 0.04	$(1.506 \pm 0.002)^2$
	-0.116 ± 0.021	-0.813 ± 0.011	0.226 ± 0.015	0.523 ± 0.006	-0.014 ± 0.014	

TABLE I: The values of mixing angles θ_a , θ_K , and the transition parameters λ_0 , λ_1 , λ_G , λ_{GG} , and mixing parameters $R_{f_0(980)NN}$, $R_{f_0(980)NS}$, $R_{f_0(980)N'}$, $R_{f_0(980)S'}$, $R_{f_0(980)G}$ for the various values of λ_{01} .

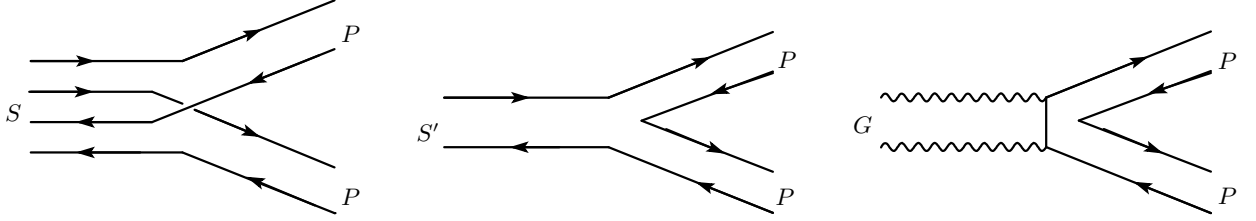


Fig 10. SPP , $S'PP$ and GPP coupling

obtained from ϕ decay, and then suggest the importance of the mixing between $qq\bar{q}\bar{q}$ and $q\bar{q}$ scalar mesons.

We use the following expressions for $S(qq\bar{q}\bar{q}$ scalar meson) PP , $S'(q\bar{q}$ scalar meson) PP and G (pure glueball) PP coupling with coupling constants A , A' and A'' , respectively [6, 8],

$$L_I = A\varepsilon^{abc}\varepsilon_{def}S_a^dP_b^eP_c^f + A'S_a^{rb}\{P_b^c, P_c^a\} + A''G\{P_a^b, P_b^a\},$$

for non-derivative coupling

$$A\varepsilon^{abc}\varepsilon_{def}S_a^d\partial^\mu P_b^e\partial_\mu P_c^f + A'S_a^{rb}\{\partial^\mu P_b^c, \partial_\mu P_c^a\} + A''G\{\partial^\mu P_a^b, \partial_\mu P_b^a\}.$$

for derivative coupling

These interactions are represented graphically by the diagrams shown in Fig. 10. We define the coupling constants $g_{SPP'}$ in the following expression,

$$\begin{aligned} L_I = & g_{a_0K\bar{K}}[\partial^\mu\bar{K}\tau\cdot\mathbf{a}_0[\partial_\mu]K + g_{a'_0K\bar{K}}[\partial^\mu\bar{K}\tau\cdot\mathbf{a}'_0[\partial_\mu]K + g_{a_0\pi\eta}\mathbf{a}_0\cdot[\partial^\mu]\pi[\partial_\mu]\eta \\ & + g_{a'_0\pi\eta}\mathbf{a}'_0\cdot[\partial^\mu]\pi[\partial_\mu]\eta + g_{a_0\pi\eta'}\mathbf{a}_0\cdot[\partial^\mu]\pi[\partial_\mu]\eta' + g_{a'_0\pi\eta'}\mathbf{a}'_0\cdot[\partial^\mu]\pi[\partial_\mu]\eta' \\ & + g_{K_0^*K\pi}([\partial^\mu]\bar{K}\tau\cdot[\partial_\mu]\pi K_0^* + H.C.) + g_{K_0^{*'}K\pi}([\partial^\mu]\bar{K}\tau\cdot[\partial_\mu]\pi K_0^{*'} + H.C.) \\ & + g_{K_0^*K\eta}(\bar{K}_0^{*'}[\partial^\mu]K[\partial_\mu]\eta + H.C.) + g_{K_0^{*'}K\eta}(\bar{K}_0^{*'}[\partial^\mu]K[\partial_\mu]\eta + H.C.) \\ & + g_{K_0^*K\eta'}(\bar{K}_0^{*'}[\partial^\mu]K[\partial_\mu]\eta' + H.C.) + g_{K_0^{*'}K\eta'}(\bar{K}_0^{*'}[\partial^\mu]K[\partial_\mu]\eta' + H.C.), \\ & + g_{f_0(M)\pi\pi}\frac{1}{2}f_0(M)[\partial^\mu]\pi\cdot[\partial_\mu]\pi + g_{f_0(M)K\bar{K}}f_0(M)[\partial^\mu]K[\partial_\mu]\bar{K} + g_{f_0(M)\eta\eta}f_0(M)[\partial^\mu]\eta[\partial_\mu]\eta \\ & + g_{f_0(M)\eta\eta'}f_0(M)[\partial^\mu]\eta[\partial_\mu]\eta' + g_{f_0(M)\eta'\eta'}f_0(M)[\partial^\mu]\eta'[\partial_\mu]\eta', \end{aligned}$$

where $[\partial^\mu]$'s are replaced to 1 for non-derivative couplings. These definitions of $g_{SPP'}$'s are the same as ones of g_{SPP} in our previous work [8] except for $g_{a_0K\bar{K}}$, $g_{K_0^*K\pi}$, which are related as $\sqrt{2}g_{a_0K\bar{K}} = \gamma_{a_0K\bar{K}}$, $\sqrt{2}g_{K_0^*K\pi} = \gamma_{K_0^*K\pi}$.

Then the coupling constants g_{SPP} 's are expressed as

$$\begin{aligned}
g_{a_0(980)K\bar{K}} &= \sqrt{2}(A \cos \theta_a - A' \sin \theta_a), \\
g_{a_0(1450)K\bar{K}} &= \sqrt{2}(A \sin \theta_a + A' \cos \theta_a), \\
g_{a_0(980)\pi\eta} &= 2(A \cos \theta_a \sin \theta_P - \sqrt{2}A' \sin \theta_a \cos \theta_P), \\
g_{a_0(1450)\pi\eta} &= 2(A \sin \theta_a \sin \theta_P + \sqrt{2}A' \cos \theta_a \cos \theta_P), \\
g_{a_0(1450)\pi\eta'} &= 2(-A \sin \theta_a \cos \theta_P + \sqrt{2}A' \cos \theta_a \sin \theta_P), \\
g_{K_0^*(800)\pi K} &= \sqrt{2}(A \cos \theta_K - A' \sin \theta_K), \\
g_{K_0^*(1430)\pi K} &= \sqrt{2}(A \sin \theta_K + A' \cos \theta_K), \\
g_{f_0(M)\pi\pi} &= 2(-AR_{f_0(M)NN} + \sqrt{2}A'R_{f_0(M)N'} + 2A''R_{f_0(M)G}),
\end{aligned} \tag{43}$$

$$\begin{aligned}
g_{f_0(M)K\bar{K}} &= \sqrt{2}(-AR_{f_0(M)NS} + A'R_{f_0(M)N'} + \sqrt{2}A'R_{f_0(M)S'} + 2\sqrt{2}A''R_{f_0(M)G}), \\
g_{f_0(M)\eta\eta} &= 2 \left(-AR_{f_0(M)NS} \cos \theta_P \sin \theta_P + \frac{1}{2}AR_{f_0(M)NN} \cos^2 \theta_P \right. \\
&\quad \left. + \frac{1}{\sqrt{2}}A'R_{f_0(M)N'} \cos^2 \theta_P + A'R_{f_0(M)S'} \sin^2 \theta_P + A''R_{f_0(M)G} \right), \\
g_{f_0(M)\eta\eta'} &= 2 \left(AR_{f_0(M)NS} \cos 2\theta_P + \frac{1}{2}AR_{f_0(M)NN} \sin 2\theta_P \right. \\
&\quad \left. + \frac{1}{\sqrt{2}}A'R_{f_0(M)N'} \sin 2\theta_P - A'R_{f_0(M)S'} \sin 2\theta_P \right), \\
g_{f_0(M)\eta'\eta'} &= 2 \left(AR_{f_0(M)NS} \cos \theta_P \sin \theta_P + \frac{1}{2}AR_{f_0(M)NN} \sin^2 \theta_P \right. \\
&\quad \left. + \frac{1}{\sqrt{2}}A'R_{f_0(M)N'} \sin^2 \theta_P + A'R_{f_0(M)S'} \cos^2 \theta_P + A''R_{f_0(M)G} \right),
\end{aligned}$$

where θ_P is the η - η' mixing angle related to the traditional octet-singlet mixing angle θ_{0-8} as $\theta_P = \theta_{0-8} + 54.7^\circ$.

Decay widths for these scalar mesons are expressed by using the coupling constant g_{SPP} as

$$\begin{aligned}
\Gamma(a_0(M) \rightarrow K^+(m_1)K^-(m_2) + K^0(m_1)\bar{K}^0(m_2)) &= 2 \frac{g_{a_0(M)K\bar{K}}^2}{8\pi} \frac{|\mathbf{q}|}{m_{a_0(M)}^2} \left[\left(\frac{m_{Mm_1m_2}^2}{2} \right)^2 \right], \\
\Gamma(a_0(M) \rightarrow \pi(m_1) + \eta(m_2)) &= \frac{g_{a_0(M)\pi\eta}^2}{8\pi} \frac{|\mathbf{q}|}{m_{a_0(M)}^2} \left[\left(\frac{m_{Mm_1m_2}^2}{2} \right)^2 \right], \\
\Gamma(a_0(M) \rightarrow \pi(m_1) + \eta'(m_2)) &= \frac{g_{a_0(M)\pi\eta'}^2}{8\pi} \frac{|\mathbf{q}|}{m_{a_0(M)}^2} \left[\left(\frac{m_{Mm_1m_2}^2}{2} \right)^2 \right], \\
\Gamma(K_0^{*+}(M) \rightarrow \pi^+(m_1)K^0(m_2) + \pi^0(m_1)K^+(m_2)) &= 3 \frac{g_{K_0^{*+}(M)\pi K}^2}{8\pi} \frac{|\mathbf{q}|}{m_{K_0^{*+}(M)}^2} \left[\left(\frac{m_{Mm_1m_2}^2}{2} \right)^2 \right], \\
\Gamma(f_0(M) \rightarrow \pi^+(m_1)\pi^-(m_2) + \pi^0(m_1)\pi^0(m_2)) &= \frac{3}{2} \frac{g_{f_0(M)\pi\pi}^2}{8\pi} \frac{|\mathbf{q}|}{m_{f_0(M)}^2} \left[\left(\frac{m_{Mm_1m_2}^2}{2} \right)^2 \right], \\
\Gamma(f_0(M) \rightarrow K^+(m_1)K^-(m_2) + K^0(m_1)\bar{K}^0(m_2)) &= 2 \frac{g_{f_0(M)K\bar{K}}^2}{8\pi} \frac{|\mathbf{q}|}{m_{f_0(M)}^2} \left[\left(\frac{m_{Mm_1m_2}^2}{2} \right)^2 \right], \\
\Gamma(f_0(M) \rightarrow \eta(m_1) + \eta(m_2)) &= 2 \frac{g_{f_0(M)\eta\eta}^2}{8\pi} \frac{|\mathbf{q}|}{m_{f_0(M)}^2} \left[\left(\frac{m_{Mm_1m_2}^2}{2} \right)^2 \right], \\
\Gamma(f_0(M) \rightarrow \eta(m_1) + \eta'(m_2)) &= \frac{g_{f_0(M)\eta\eta'}^2}{8\pi} \frac{|\mathbf{q}|}{m_{f_0(M)}^2} \left[\left(\frac{m_{Mm_1m_2}^2}{2} \right)^2 \right], \\
\Gamma(f_0(M) \rightarrow \eta'(m_1) + \eta'(m_2)) &= 2 \frac{g_{f_0(M)\eta'\eta'}^2}{8\pi} \frac{|\mathbf{q}|}{m_{f_0(M)}^2} \left[\left(\frac{m_{Mm_1m_2}^2}{2} \right)^2 \right].
\end{aligned} \tag{44}$$

Here $|\mathbf{q}|$ and $m_{Mm_1m_2}$ are defined as

$$\begin{aligned}
|\mathbf{q}| &= \sqrt{\left(\frac{M^2 + m_2^2 - m_1^2}{2M} \right)^2 - m_2^2}, \\
m_{Mm_1m_2} &= \sqrt{M^2 - m_1^2 - m_2^2},
\end{aligned}$$

and for the case $M \approx m_1 + m_2$, we use the next formula for $|\mathbf{q}|$ [11],

$$|\mathbf{q}| = \text{Re} \frac{1}{\sqrt{2\pi}\Gamma_M} \int_{M-\infty}^{M+\infty} e^{-\frac{(m-M)^2}{2\Gamma_M^2}} \times \sqrt{\left(\frac{M^2 + m_2^2 - m_1^2}{2M} \right)^2 - m_2^2} dm, \tag{45}$$

where Γ_M is the decay width of particle with mass M .

We use the experimental data of the scalar meson decays cited in Ref. [5]; $\Gamma(a_0(980) \rightarrow \pi\eta + K\bar{K}) = 75 \pm 25 \text{MeV}$, $\Gamma(a_0(1450) \rightarrow \pi\eta + \pi\eta' + K\bar{K}) = 265 \pm 13 \text{MeV}$, $\Gamma(K_0^*(1430) \rightarrow \pi K) = 270 \pm 43 \text{MeV}$ [12], $\Gamma(f_0(980) \rightarrow \pi\pi + K\bar{K}) = 70 \pm 30 \text{MeV}$, $\Gamma(f_0(1370) \rightarrow \pi\pi + K\bar{K} + \eta\eta) = 214 \pm 120 \text{MeV}$ [13], $\Gamma(f_0(1500) \rightarrow \pi\pi + K\bar{K} + \eta\eta + \eta\eta') = 55 \pm 9 \text{MeV}$ [14], $\Gamma(f_0(1710) \rightarrow \pi\pi + K\bar{K} + \eta\eta) = 137 \pm 8 \text{MeV}$, for the best fitting of our model parameters, A , A' , A'' and θ_P . Results are tabulated in Table II for non-derivative coupling case and in Table III for derivative coupling case. For the θ_P , we search the best fit value in the range $(54.7 \pm 18)^\circ$. We estimate the best fit values of these parameters for various points (0.2, 0.25, 0.30, 0.35, 0.40, 0.45) GeV^2 of inter-mixing parameter λ_{01} . We show the values of $\Gamma(a_0(980) \rightarrow \pi\eta + K\bar{K})$ etc. and $g_{a_0(980)\pi\eta}$ etc. for best fitted A , A' , A'' and θ_P . Values in the row just below the one denoting $\Gamma(a_0(980) \rightarrow \pi\eta + K\bar{K})$ etc. denote the experimental values and the values in the row just below the one denoting $g_{a_0(980)\pi\eta}$ etc. are the values Eqs. (18), (18'), (27), (27') obtained from $\phi \rightarrow a_0\gamma/\pi^0\eta\gamma$ and $\phi \rightarrow f_0\gamma/\pi^0\pi^0\gamma$ decay analyses.

These results in Table II (non-derivative coupling case) show that the values of $g_{a_0(980)\pi\eta}$ etc. obtained for $\lambda_{01} = 0.30 \sim 0.35 (\text{GeV}^2)$ are close to the values obtained in $\phi \rightarrow a_0\gamma/\pi^0\eta\gamma$ and $\phi \rightarrow f_0\gamma/\pi^0\pi^0\gamma$ decay analyses. For the derivative coupling case (showed in Table III), the values of $g_{a_0(980)\pi\eta}$ etc. except for $g_{f_0(980)K\bar{K}}$ obtained for $\lambda_{01} = 0.30 \sim 0.35 (\text{GeV}^2)$ are also close to the values obtained in $\phi \rightarrow a_0\gamma/\pi^0\eta\gamma$ and $\phi \rightarrow f_0\gamma/\pi^0\pi^0\gamma$ decay analyses. But characteristic feature $g_{f_0(980)K\bar{K}}/g_{a_0(980)K\bar{K}} \sim 2$ obtained in $\phi \rightarrow a_0\gamma/\pi^0\eta\gamma$ and $\phi \rightarrow f_0\gamma/\pi^0\pi^0\gamma$ decay analyses cannot be taken in any values of λ_{01} for derivative coupling case..

$\lambda_{01}(\text{GeV}^2)$	A	A'	A''	θ_P	$\Gamma_{a_0(980) \rightarrow \pi\eta + K\bar{K}}$
	GeV	GeV	GeV	degree($^\circ$)	$0.075 \pm 0.025 \text{ GeV}$
0.20	2.8	1.2	-0.25	36.7	0.189
0.25	2.5	1.2	-0.23	36.7	0.133
0.30	2.3	1.2	-0.24	36.7	0.097
0.35	1.9	1.3	-0.24	50.2	0.081
0.40	1.7	1.3	-0.24	59.2	0.072
0.45	1.5	1.4	-0.26	72.7	0.068
	$\Gamma_{a_0(1450) \rightarrow \pi\eta + \pi\eta' + K\bar{K}}$	$\Gamma_{K_0^*(1430) \rightarrow \pi K}$	$\Gamma_{f_0(980) \rightarrow \pi\pi + K\bar{K}}$	$\Gamma_{f_0(1370) \rightarrow \pi\pi + K\bar{K} + \eta\eta}$	$\Gamma_{f_0(1500) \rightarrow \pi\pi + K\bar{K} + \eta\eta + \eta\eta'}$
	$0.265 \pm 0.013 \text{ GeV}$	$0.270 \pm 0.043 \text{ GeV}$	$0.070 \pm 0.030 \text{ GeV}$	$0.214 \pm 0.120 \text{ GeV}$	$0.055 \pm 0.009 \text{ GeV}$
0.20	0.242	0.192	0.119	0.034	0.063
0.25	0.250	0.204	0.107	0.031	0.057
0.30	0.258	0.214	0.104	0.029	0.055
0.35	0.273	0.232	0.098	0.034	0.058
0.40	0.263	0.233	0.098	0.040	0.054
0.45	0.272	0.253	0.124	0.084	0.056
	$\Gamma_{f_0(1710) \rightarrow \pi\pi + K\bar{K} + \eta\eta}$	$g_{a_0(980) K\bar{K}}$	$g_{a_0(980) \pi\eta}$	$g_{f_0(980) K\bar{K}}$	$g_{f_0(980) \pi\pi}$
	$0.137 \pm 0.008 \text{ GeV}$	$2.18 \pm 0.12 \text{ GeV}$	$1.89 \pm 0.75 \text{ GeV}$	$4.72 \pm 0.82 \text{ GeV}$	$1.12 \pm 0.69 \text{ GeV}$
0.20	0.177	3.62	2.84	4.51	0.31
0.25	0.156	3.09	2.34	4.21	0.45
0.30	0.140	2.70	1.95	4.05	0.61
0.35	0.151	2.00	2.06	3.74	0.78
0.40	0.129	1.59	2.06	3.63	1.00
0.45	0.141	1.12	2.13	3.66	1.27

TABLE II: The results of the best fit analyses for non-derivative coupling case. The experimental data of the scalar meson decay widths used are cited in Ref. [5]. For the θ_P , we search the best fit value in the range $(54.7 \pm 18)^\circ$. The values of $g_{a(980)\pi\eta}$ etc. are ones obtained for $\phi \rightarrow a_0(980)\gamma/\pi^0\eta\gamma$ and $\phi \rightarrow f_0(980)\gamma/\pi^0\pi^0\gamma$ decay analysis.

V. CONCLUSION

From the invariant mass distribution analysis of radiative decays $\phi \rightarrow a_0(980)\gamma \rightarrow \pi^0\eta\gamma$ and $\phi \rightarrow f_0(980)\gamma \rightarrow \pi^0\pi^0\gamma$, we obtain the results that the $K\bar{K}$ loop diagram contribution for $\phi a_0\gamma$ and $\phi f_0\gamma$ couplings are dominant for both non-derivative and derivative SPP coupling cases. We assume that $\phi \rightarrow a_0(980)\gamma$ and $\phi \rightarrow f_0(980)\gamma$ decays are caused through only the $K\bar{K}$ loop diagram, and then we get the results Eqs. (18), (18'), (27), (27') of SPP coupling constants,

	non-derivative coupling	derivative coupling
$g_{aK\bar{K}}$	$2.18 \pm 0.12 \text{ GeV}$	$9.04 \pm 0.50 \text{ GeV}^{-1}$
$g_{a_0\pi\eta}$	$1.89 \pm 0.75 \text{ GeV}$	$5.79 \pm 2.32 \text{ GeV}^{-1}$
$g_{fK\bar{K}}$	$4.72 \pm 0.82 \text{ GeV}$	$20.0 \pm 0.50 \text{ GeV}^{-1}$
$g_{f_0\pi\pi}$	$1.12 \pm 0.69 \text{ GeV}$	$2.43 \pm 1.50 \text{ GeV}^{-1}$

We consider that the scalar $a_0(980)$ and $f_0(980)$ are $q\bar{q}q\bar{q}$ states and mix with high mass scalar mesons considered as $q\bar{q}$ states. The low mass scalar and high mass scalar mesons are considered to mix through the inter-mixing parameter λ_{01} . In our mass formula, we obtain the mixing angle θ_a , θ_K and mixing parameters $R_{f_0(980)NN}$'s using the mass values of low mass scalar mesons ($a_0(980)$, $K_0^*(800)$, $f_0(600)$, $f_0(980)$) and high mass scalar mesons and glueball ($a_0(1450)$, $K_0^*(1430)$, $f_0(1370)$, $f_0(1500)$, $f_0(1710)$). We tabulate these values for $\lambda_{01} = (0.30 \leftrightarrow 0.35) \text{ GeV}^2$.

$$\theta_a = (15.0 \leftrightarrow 17.8)^\circ, \quad \theta_K = (13.8 \leftrightarrow 16.4)^\circ, \quad ,$$

$\lambda_{01}(\text{GeV}^2)$	A	A'	A''	θ_P	$\Gamma_{a_0(980) \rightarrow \pi\eta + K\bar{K}}$
	GeV^{-1}	GeV^{-1}	GeV^{-1}	degree($^\circ$)	$0.075 \pm 0.025 \text{GeV}$
0.20	5.8	1.2	-0.26	41.2	0.093
0.25	8.3	0.57	-0.37	36.7	0.170
0.30	7.2	0.51	-0.33	36.7	0.124
0.35	6.0	0.54	-0.35	36.7	0.068
0.40	5.1	0.57	-0.36	36.7	0.054
0.45	4.2	0.59	-0.34	50.2	0.051
	$\Gamma_{a_0(1450) \rightarrow \pi\eta + \pi\eta' + K\bar{K}}$	$\Gamma_{K_0^*(1430) \rightarrow \pi K}$	$\Gamma_{f_0(980) \rightarrow \pi\pi + K\bar{K}}$	$\Gamma_{f_0(1370) \rightarrow \pi\pi + K\bar{K} + \eta\eta'}$	$\Gamma_{f_0(1500) \rightarrow \pi\pi + K\bar{K} + \eta\eta + \eta\eta'}$
	$0.265 \pm 0.013 \text{GeV}$	$0.270 \pm 0.043 \text{GeV}$	$0.070 \pm 0.030 \text{GeV}$	$0.214 \pm 0.120 \text{GeV}$	$0.055 \pm 0.009 \text{GeV}$
0.20	0.276	0.239	0.025	0.009	0.057
0.25	0.274	0.262	0.045	0.083	0.068
0.30	0.279	0.267	0.036	0.099	0.053
0.35	0.279	0.266	0.028	0.090	0.055
0.40	0.279	0.266	0.025	0.082	0.059
0.45	0.276	0.246	0.022	0.056	0.057
	$\Gamma_{f_0(1710) \rightarrow \pi\pi + K\bar{K} + \eta\eta}$	$g_{a_0(980)K\bar{K}}$	$g_{a_0(980)\pi\eta}$	$g_{f_0(980)K\bar{K}}$	$g_{f_0(980)\pi\pi}$
	$0.137 \pm 0.008 \text{GeV}$	$9.04 \pm 0.50 \text{GeV}^{-1}$	$5.79 \pm 2.32 \text{GeV}^{-1}$	$20.0 \pm 3.48 \text{GeV}^{-1}$	$2.43 \pm 1.50 \text{GeV}^{-1}$
0.20	0.158	7.80	7.10	8.63	0.39
0.25	0.106	11.3	9.42	11.6	0.65
0.30	0.152	9.65	8.02	9.94	0.87
0.35	0.152	7.85	6.45	8.23	1.03
0.40	0.152	6.45	5.24	6.94	1.28
0.45	0.132	5.07	5.45	5.67	1.39

TABLE III: The results of the best fit analyses for derivative coupling case. The experimental data of the scalar meson decay widths used are cited in Ref. [5]. For the θ_P , we search the best fit value in the range $(54.7 \pm 18)^\circ$. The values of $g_{a_0(980)\pi\eta}$ etc. are ones obtained for $\phi \rightarrow a_0(980)\gamma/\pi^0\eta\gamma$ and $\phi \rightarrow f_0(980)\gamma/\pi^0\pi^0\gamma$ decay analysis.

	f_{NN}	f_{NS}	$f_{N'}$	$f_{S'}$	f_G
$f_0(600)$	$-0.98 \leftrightarrow -0.97$	$0.05 \leftrightarrow 0.07$	$0.20 \leftrightarrow 0.23$	$-0.06 \leftrightarrow -0.08$	$-0.00 \leftrightarrow -0.01$
$f_0(980)$	$-0.05 \leftrightarrow -0.07$	$-0.93 \leftrightarrow -0.90$	$0.11 \leftrightarrow 0.14$	$0.34 \leftrightarrow 0.40$	~ -0.02
$f_0(1370)$	$0.13 \leftrightarrow 0.16$	$-0.25 \leftrightarrow -0.29$	$0.48 \leftrightarrow 0.49$	$-0.83 \leftrightarrow -0.80$	~ 0.02
$f_0(1500)$	$-0.02 \leftrightarrow -0.03$	$-0.03 \leftrightarrow -0.05$	$-0.09 \leftrightarrow -0.10$	$-0.02 \leftrightarrow -0.03$	~ 0.99
$f_0(1710)$	$-0.16 \leftrightarrow -0.19$	$-0.25 \leftrightarrow -0.30$	$-0.85 \leftrightarrow -0.82$	$-0.44 \leftrightarrow -0.43$	$-0.10 \leftrightarrow -0.12$

The fact that $f_0(980)$ state considered as the f_{NS} state mainly has the rather large $f_{S'}$ component with sign opposite to the f_{NS} one suggests a possibility that $g_{f_0K\bar{K}}/g_{a_0K\bar{K}}$ can be about 2, because $g_{f_0K\bar{K}}/g_{a_0K\bar{K}} = |(-AR_{f_0NS} + A'R_{f_0N'} + \sqrt{2}A'R_{f_0S'} + A''R_{f_0G})/(A\cos\theta_a - A'\sin\theta_a)|$ and $\theta_a > 0$. In our model, $f_0(1500)$ meson is considered as glueball, and $f_0(1370)$ meson is almost $f_{S'}$ state with rather large $f_{N'}$ component and $f_0(1710)$ meson is almost $f_{N'}$ state with rather large $f_{S'}$ component.

Because $g_{f_0K\bar{K}}$'s are related to the mixing parameters R_{f_0NS} 's and coupling strengths A, A', A'' and η - η' mixing angle θ_P , we executed the best fit analyses of the various SPP decays in the wide range of the λ_{12} value for non-derivative and derivative coupling cases. The best fit values of A 's and $g_{a_0K\bar{K}}$'s are tabulated in Table II and III. These results suggest that the non-derivative coupling seems to be reasonable than the derivative one and the inter-mixing parameter λ_{12} is rather large $0.30 \leftrightarrow 0.35$.

-
- [1] N. N. Achasov and V. N. Ivanchenko, Nucl. Phys. **B315**, 465(1989).
F. E. Close and N. Isgur and S. Kumano, Nucl. Phys. **B389**, 513(1993).
N. N. Achasov, V. V. Gubin, and V. I. Shevchenko, Phys. Rev. **D56**, 203(1997).
[2] N. N. Achasov and V. V. Gubin, Phys. Rev. **D56**, 4084(1997).
R. Delbourgo, Dongsheng Liu, M. D. Scadron, Phys. Lett. **B446**, 332(1999).
N. N. Achasov Nucl. Phys. **A675**, 279c(2000).

- [3] D. Black, M. Harada and J. Schechter, Phys. Rev. D **73**, 054017(2006) [arXiv:hep-ph/0601052].
- [4] M. N. Achasov *et al.* [SND Collaboration], Phys. Lett. B **479**, 53(2000).
R. R. R. Akhmetshin *et al.* [CMD-2 Collaboration], Phys. Lett. B **462**, 371, i-bid. 380(1999).
A. Alosio *et al.* [KLEO Collaboration], Phys. Lett. B **536**, 209(2002); Phys. Lett. B **537**, 21(2002).
- [5] W.-M. Yao *et al.* (Particle Data Group), J. Phys. G **33**, 1(2006).
- [6] D. Black *et al.*, Phys. Rev. D **59**, 074026(1999);
D. Black, A. H. Fariborz and J. Schechter, Phys. Rev. D **61**, 074001(2000).
- [7] T. Teshima, I. Kitamura and N. Morisita, J. Phys. G: Nucl. Part. Phys. **28**, 1391(2002).
- [8] T. Teshima, I. Kitamura and N. Morisita, J. Phys. G **30**, 663(2004).
- [9] T. Teshima, I. Kitamura and N. Morisita, Nucl. Phys. A **759**, 131 (2005).
- [10] R. J. Jaffe, Phys. Rev. D **15**, 267(1977).
M. Alford and R. L. Jaffe, Nucl. Phys. B **578**, 367(2000).
- [11] M. Harada, F. Sannio and J. Schechter, Phys. Rev. D **54**, 1991(1996).
- [12] D. Aston *et al.*, Nucl. Phys. B **296**, 493(1988).
- [13] D. V. Bugg, A. V. Sarantsev and B. S. Zou, Nucl. Phys. B **471**, 59(1996).
- [14] C. Amsler *et al.*, Euro. Phys. J. C **23**, 29(2002); Phys. Lett. B **353**, 571(1995).
D. Barberis *et al.*, Phys. Lett. B **471**, 429(2000); Phys. Lett. B **479**, 59(2000).
D. V. Bugg, A. V. Sarantsev and B. S. Zou, Nucl. Phys. B **471**, 59(1996).